Desalination and Water Treatment
www.deswater.com
doi: 10.1080/19443994.2014.976770

57 (2016) 1790–1803
January

Taylor & Francis
Taylor & Francis Group

Development and application of Palygorskite porous ceramsite in a biological aerated filter (BAF)

Teng Bao[a,b], Tian-hu Chen[a,*], Chengsong Qing[a], Jin Jin Xie[a], Ray L. Frost[b]

[a]*Laboratory for Nanominerals and Environmental Material, School of Resource and Environmental Engineering, Hefei University of Technology, Hefei, China, email: chentianhu@hfut.edu.cn*
[b]*School of Chemistry, Physics and Mechanical Engineering, Science and Engineering Faculty, Queensland University of Technology, Brisbane, Australia*

Received 2 April 2014; Accepted 1 October 2014

ABSTRACT

Novel filter Palygorskite porous ceramsite (PC) was prepared using Palygorskite clay, pore-forming material sawdust, and sodium silicate with a mass ratio of 10:2:1 after sintering at 700°C for 180 min. PC was characterized with X-ray diffraction, X-ray fluorescence, scanning electron microscopy, elemental, and porosimetry. PC had a total porosity of 67% and specific surface area of 61 m^2/g. In order to assess the usefulness of PC as a medium for biological aerated filters (BAF), PC and (commercially available ceramsite) CAC were used to treat wastewater city in two laboratory-scale upflow BAFs. The results showed that the reactor containing PC was more efficient than the reactor containing CAC in terms of total organic carbon (TOC), ammonia nitrogen (NH_3-N), and the removal of total nitrogen (TN) and phosphorus (P). This system was found to be more efficient at water temperatures ranging from 20 to 26°C, an air–water (A/W) ratio of 3:1, dissolved oxygen concentration >4.00 mg/L, and hydraulic retention time (HRT) ranging from 0.5 to 7 h. The interconnected porous structure produced for PC was suitable for microbial growth, and primarily protozoan and metazoan organisms were found in the biofilm. Microorganism growth also showed that, under the same submerged culture conditions, the biological mass in PC was significantly higher than in CAC (34.1 and 2.2 mg TN/g, respectively). In this way, PC media can be considered suitable for the use as a medium in novel biological aerated filters for the simultaneous removal of nitrogen and phosphorus.

Keywords: Palygorskite porous ceramsite; Simultaneous nitrification and denitrification; Simultaneous removal of nitrogen and phosphorus; Biofilm

1. Introduction

The accumulation of nutrients in surface waters, especially nitrogen and phosphorus, can lead to the deterioration of water quality, such as the formation of algal bloom, which can in turn cause blooms of aquatic plants and depletion of dissolved oxygen from eutrophication [1,2]. Phosphorus is an important nutrient. It is a nonrenewable resource and contributes to eutrophication. Phosphorus removal from wastewater has been widely studied during the past decades [3]. There is a need to develop wastewater treatment processes that allow the reuse of phosphorus. In order to control the nutrient enrichment in watersheds,

*Corresponding author.

1944-3994/1944-3986 © 2014 Balaban Desalination Publications. All rights reserved.

various types of operational systems have been tested by wastewater treatment plants. These methods focus on the simultaneous removal of nitrogen and phosphorus from municipal wastewater [4,5].

A biological aerated filter (BAF) is a flexible bioreactor that provides a small-footprint option for the processing of wastewater at various stages [6–10]. Media selection is critical to the design and operation of BAFs that meet effluent quality requirements [11–14]. The selection of granular media plays an important role in the maintenance of large amounts of active biomass and diverse microbial populations. So far, the most frequently studied BAF support media have been clay-, schist-, and plastic-based varieties such as polyethylene and polystyrene [15,16]. However, the bioactivity and contaminant removal efficiencies of BAF are usually low because most medium materials have poor affinity for biofilm growth and low surface hydrophilicity and biocompatibility. Several new medium materials have been developed for the use in BAF systems to enhance their biodegradation capability [17,18]. For example, Liu et al. investigated the performance of the BAF in an oyster shell and a plastic ball as a carrier media [19]. They reported that the average removal rates of COD and ammonia increased up to over 80% and 94%, respectively, when (hydraulic retention time) HRT exceeded 4 h. Han et al. investigated the performance of a BAF with fly ash ceramic particles and commercial ceramic particles (CCP) [20]. They reported that SFCP reactor was more effective than the CCP reactor in terms of total nitrogen (TN) removal at the optimum C/N ratio of 4.03 when volumetric loading rates (VLRs) ranged from 0.33 to 3.69 kg TN (m^3/d). Both materials achieved good results for nitrogen removal but did not focus on phosphorus removal. There is a need to investigate the simultaneous removal of both nutrients.

In chemical treatment, a divalent or trivalent metal salt is added to wastewater. This causes precipitation of an insoluble metal phosphate, which settles out by sedimentation. The salts most commonly used in the presence of chlorides and sulfates are iron and aluminum. Lime is also used because of the formation of calcium phosphate. However, those methods generally produce a large amount of excess sludge with a high water content. This sludge is hard to dispose of and causes secondary contamination [21,22].

Palygorskite is an aluminum-magnesium silicate with a fibrous morphology. Its structure was first reported by Bradlely [23]. Its physicochemical characteristics make it an attractive adsorbent. Recently, its use as an environmental adsorbent has gained attention. Its adsorption capacity can be increased by modifying its texture by means of chemical or thermal treatments. This does not cause the loss of any other physicochemical property [24–26]. However, there have been few studies on the removal of phosphate ions from water using Palygorskite.

In this study, Palygorskite was selected as one of the raw materials for the synthesis of a novel particle-Palygorskite porous ceramsite (PC) filter medium for the simultaneous removal of nitrogen and phosphorus filter media. Sawdust is a by-product of timber processing and extraction. In China, the annual production of has reached nearly 180 million tons and is increasing at an annual rate of 6-8%. The generation of sawdust has resulted in considerable accumulation in many places throughout China. The management of sawdust waste places a heavy economic burden on industry [27,28]. Finding a use for waste sawdust would have a considerable impact. Lu et al. have reported that, at high sintering temperatures, the lignin and cellulose in sawdust can be converted into a porous, carbonaceous material that can be used as a cellular material [29]. To the best of our knowledge, only a few studies have been conducted on the use of sawdust as a porous material. The fact that some waste materials, such as ceramsite and polyethylene plastic, have been successfully used as filter media for BAFs suggests a new approach to the reuse of sawdust [30].

In this study, Palygorskite, sawdust, and sodium silicate were used as the main materials for the fabrication of a novel of PC for the simultaneous removal of nitrogen and phosphorus. These particles were used as biofilm supports in a BAF, and their effectiveness in wastewater treatment was compared to that of commercially available ceramsite (CAC). The optimal preparation conditions of PC were determined through orthogonal testing. The objective of this paper was to investigate the effect of hydraulic retention time (HRT) on the removal of total organic carbon (TOC), ammonia nitrogen (NH_3-N), total nitrogen (TN), and phosphorus (P) in the two BAF systems. The apparent properties of PC and CAC, and the microbial characteristics of the two systems were analyzed using various characterization and analytical techniques. The feasibility of using PC as filter medium is discussed according to the experimental results.

2. Materials and methods

2.1. Materials

Raw Palygorskite was obtained from Crown Hill, Mingguang City, Anhui Province, China. Sawdust was obtained from Hefei City, Anhui Province, China. Commercially available ceramsite was obtained from

Ma'anshan City, Anhui Province, China. Sodium silicate (solid content 70%) was obtained from Hefei Chemical Reagent Corporation (China).

Palygorskite clay was the main component of the PC tested. Sodium silicate and sawdust were used as additives and mixed with Palygorskite clay to make the new type filter media.

Five factors were considered in the PC preparation: Palygorskite clay dosage, ratio of sodium silicate added, ratio of sawdust added, calcination temperature, and calcination time.

The ratio of sodium silicate added and sawdust added both depended on the Palygorskite clay dosage. Orthogonal tests were used to analyze the influence of the five factors on the properties of PC. The experimental conditions for the preparation of PC are shown in Tables 1 and 2.

An orthogonal $L_9 4^3$ test was used for optimization of the particle preparation conditions. The evaluation index was analyzed statistically. The orthogonal test designs are listed in Table 1. Because we could not select the best preparation conditions based only on the outcomes in Table 2(a) further orthogonal analysis was warranted. The K_{mn} and R_n values were calculated and are listed in Table 2. The influence on the comprehensive index of PC was in the following order, from the greatest to the least: ratio of sodium silicate added > ratio of sawdust added > calcination temperature > calcination time. The Palygorskite clay was found to be the most important determinant of effectiveness. The optimal preparation conditions of Palygorskite were 100 g of sodium silicate added in an amount of 10 wt%, sawdust added in an amount of 20 wt%, a calcination temperature of 700˚C and a calcination time of 3 h. This formula met the Chinese national standards for PC and CAC (Table 3) [31]. Images of as-synthesized PC (left) and calcined (right) PC photographs are shown in Fig. 2.

Table 1
Factors and levels of the design of orthogonal experiments

A	B	C	D	E
1	10	20	500	1
2	11	30	600	2
3	12	40	700	3

Notes: The proportion of sodium silicate and sawdust is accounted for in the relative palygorskite content.(A) Level; (B) amount of sodium silicate (wt%Pg); (C) amount of sawdust (wt% Pg); (D) calcination temperature (˚C); (E) Calcination time (*h*).

Table 2
Results of orthogonal experiments

A	B	C	D	E	F
1	1	1	1	1	57.40
2	1	2	2	2	52.58
3	1	3	3	3	59.46
4	2	1	2	3	48.32
5	2	2	3	1	28.72
6	2	3	1	2	33.40
7	3	1	3	2	54.00
8	3	2	1	3	46.12
9	3	3	2	1	23.00
K_1	56.48	53.24	45.64	36.37	–
K_2	36.81	42.47	41.30	46.66	–
K_3	41.4	38.62	47.39	51.30	–
R	19.67	14.62	6.09	14.39	–

Notes: K_i here refers to levels of compression strength and R is the difference between the largest average effect and minimum average effect for every factor. A) Orthogonal experiment ID number; B) sodium silicate (wt%Pg); C) sawdust (wt% Pg); D) calcination temperature (˚C); E) calcination time (*h*); F) compression strength (*N*).

2.2. Applicability of PC in a BAF relative to that of CAC

2.2.1. Reactor design and start-up of BAFs

Two laboratory-scale biofilter columns were constructed from polyvinylchloride pipes that were 6 cm in diameter with a depth capable of holding 150 cm of carrier. The setups are shown in Fig. 1. Air was introduced into the reactor with an air diffuser and the air flow rate was monitored with an air flow meter. Under optimum conditions, the air flow rate was set at 2.0 L/min. The interior walls of the columns were coated with glass cement to prevent edge effects resulting from preferential flow paths down the sides of the column. The influent wastewater (including municipal wastewater) was evenly filled into a network of distribution holes at the bottom of the biofilter column. The treated effluent was collected through pipes at the top of the column.

There were two BAFs, of which one was packed with PC and the other with CAC. The raw wastewater was pumped into the two BAFs with peristaltic pumps and flowed upward through the filter media layer.

2.2.2. Operating conditions

Each test was divided into four stages. During each test stage, the operating conditions of two BAFs were identical. They are summarized in Table 4. The air–water ratio was (A/W):3:1 (DO > 4.00 mg/L).

Table 3
Regulatory levels of ceramics in PC and CAC and corresponding Chinese National Standards

Item	Chinese National Standard	PC experimental levels	CAC experimental levels
Grain diameter (d, mm)	0.5–9.0	5–8	4–6
Silt carrying capacity (C_s, %)	≤ 1	0.27	≤ 1
Solubility in hydrochloric acid (C_{ha}, %)	≤ 2	0.434	≤ 1.5
Void fraction (υ, %)	≥ 40	71.48	> 42
Specific surface area (S_w, cm^2/g)	$\geq 0.5\times10^4$	6.1×10^5	$\geq 2\times10^4$
Piled density (ρ_p, g/cm^3)	–	0.53	≤ 1.0
Apparent density (ρ_{ap}, g/cm^3)	–	1.71	1.4–1.8
Compression strength (N)	–	50–58	≥ 87
Porosity (P, %)	–	67	–

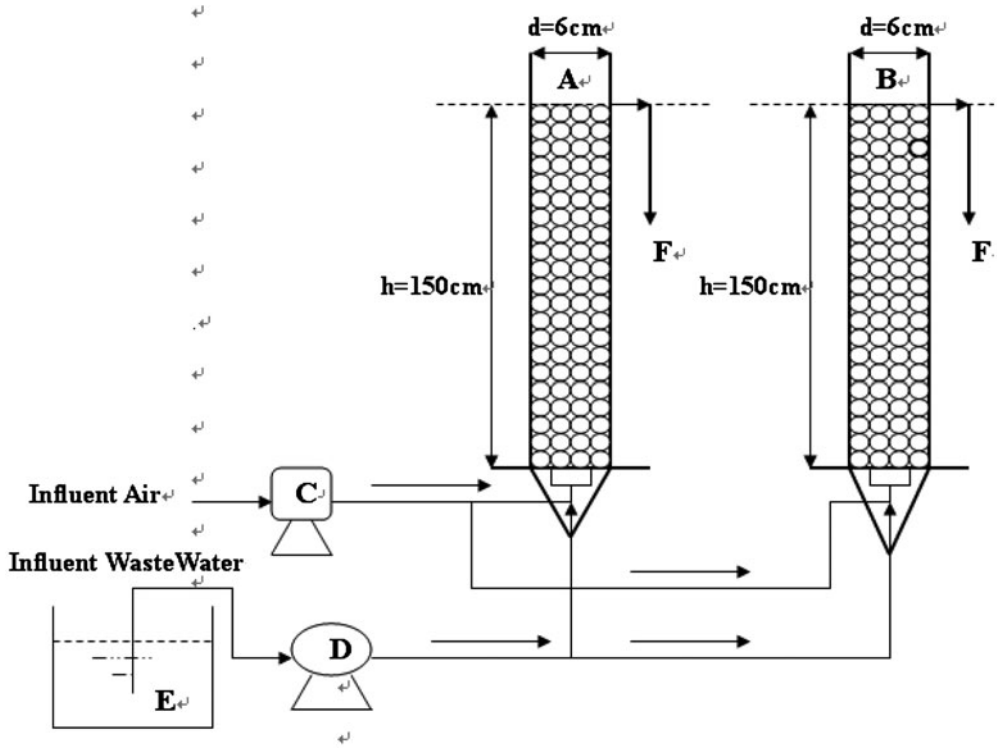

Fig. 1. Schematic diagram of the BAF system. (A) CAC BAF; (B) PC BAF; (C) air blower; (D) water pump; (E) wastewater tank; (F)effluent pipe.

2.2.3. Characterization methods

The multipoint BET (Brunauer, Emmett and Teller) surface area of PC was measured using a Quantachrome Nova 3000e automated surface area analyzer. X-ray fluorescence (XRF) chemical composition was measured on a Shimadzu XRF-1800 with Rh radiation. X-ray diffraction was performed using a Rigaku powder diffractometer with Cu Kα radiation. The tube voltage was 40 kV and the current was 100 mA. The XRD diffraction patterns were taken in the range of 5–70˚C at a scan speed of 4˚ min^{-1}. Phase identification (Search-Match) was carried out by comparison with those included in the Joint Committee of Powder Diffraction Standards (JCPDS) database.

Elemental analyses of the sample were carried out using a VARIO ELIII analyzer (Elemental Analysis System Co. Ltd, Germany). Compressive strength analyses of the sample were carried out using a KC-2a Analyzer (China).

Fig. 2. Composite particles (left) and PC (right). (a) Composite particles; (b) Palygorskite porous ceramsite (PC).

The growth of biofilm was determined according methods available in the literature [32–34]. The physical characteristics of the PC samples were measured in accordance with the sandstone pore structure method of image analysis [35].

2.2.4. Wastewater characteristics and analysis of water quality

Water samples were collected from the inlet and outlet pipes of the BAF. All the samples were stored at 0℃ for less than 24 h before the water quality was measured. Chinese EPA standard methods were used for chemical determinations [36]. The potassium dichromate method was used to measure total organic carbon (TOC). A colorimetric method was used for ammonia nitrogen (NH_3-N), total nitrogen (TN), nitrite (NO_2-N), and nitrate (NO_3-N) analysis. The dissolved oxygen (DO) concentration was measured with a portable digital DO meter (Oxi-315, China). All chemical reagents were of analytical grade and purchased from the Hefei Chemical Reagent Corporation (China).

2.2.5. Analysis of microbial diversity

PC and CAC samples were individually taken from the biofilters and treated with glutaraldehyde 3% solution buffered with 0.1 M sodium phosphate to fix the cells. This was followed by dehydration in ethanol using a critical point dryer mounted on aluminum stubs using double-sided tape and then sputter-coating with Au [37,38]. Micrographs were also obtained using a Philips XL30 environmental scanning electron microscope (ESEM) at an accelerating voltage of 40 kV. Biofilm communities in the biofilter systems were determined by removing the PC and CAC at a determined depth (75 cm from the top surface of the PC and CAC) and then diluting these samples with 0.45 μm filtered water to a final volume of 20 mL. Twenty-five microliter doses of these solutions were placed on slide glass. The microscopic observation of protozoan and metazoan population development was carried out using a U-RFL-T Olympus Biological Microscope (Japan). Species identification was accomplished by referencing the work of Shen and Zhang [39]. A method that combines the dilution plate method and the streak plate method was used for the separation and purification of culture in the biofilm samples. The identification of bacterial strains was first conducted using Gram staining. Further identification was done by observing the morphology (shape, size, color, luster, visibility, and edge status) of a colony. Replicate biofilm samples were also collected from the systems to achieve statistical soundness [40].

3. Results and discussion

3.1. X-ray diffraction

Fig. 3 shows the X-ray diffraction (XRD) patterns of as-synthesized PC and calcined PC at 700℃. The main minerals in the as-synthesized PC include quartz (SiO_2), Palygorskite, and dolomite (Fig. 3(A)). In contrast, the main minerals of calcined PC (Fig. 3(B)) are quartz (SiO_2) and Palygorskite. The reflections at $2\theta = 9.8$, 22.3, 27, and 32° were identified as PC relative to the standard JCPDS (89-6538). A new reflection at $2\theta = 26°$ was also found and identified as quartz. This may indicate that heat treatment led to a decrease in the concentration of impurities and higher crystallinity

Table 4
Operating conditions

	Operating conditions			Water quality indexes		
Sample	pH	*T* (℃)	HRT (h)	TOC (mg/L)	NH_4^+-N (mg/L)	*P* (mg/L)
Stage one	6.5 (±0.5)	25–30℃	7 (±0.5)	26–31	9.91–10.05	0.51–0.58
Stage two	6.1 (±0.5)	25–30℃	3.5 (±0.8)	27–33	9.82–10.32	0.49–0.60
Stage three	6.7 (±0.5)	20–25℃	1.75 (±0.5)	25–30	9.67–10.23	0.46–0.53
Stage four	6.9 (±0.5)	18–23℃	0.5 (±0.1)	24–38	9.65–10.45	0.53–0.58

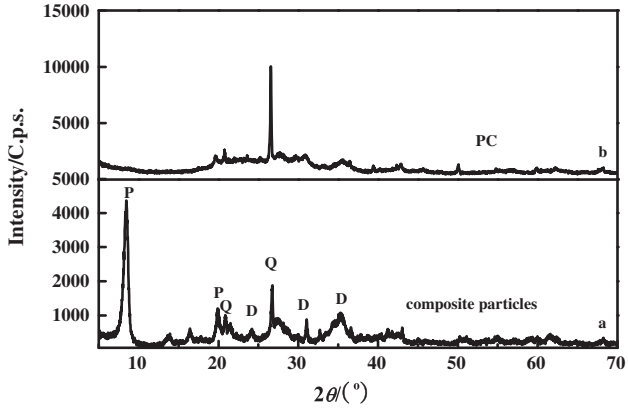

Fig. 3. X-ray diffraction patterns of composite particles and PC. (a) Composite particles; (b) calcined composite particles at 700˚C (P-Palygorskite; Q-quartz; D-dolomite).

of the material because heat treatment is also a key parameter in the improvement of specific surface area.

The characteristic diffraction peaks of dolomite and Palygorskite completely disappeared in the sample calcinated at 700˚C, but not in the as-synthesized PC. Most dolomite disappeared after thermal treatment, and the dehydroxylation of Palygorskite at 700˚C caused pore structure to collapse and destroyed the crystal structure, rendering the substance amorphous. Because dolomite was not removed completely during thermal treatment, reactions between Palygorskite and dolomite residue produced new components of MgO and Ca_2SiO_4 when calcinated at 700˚C [41].

3.2. X-ray fluorescence (XRF) and elemental analysis (EA)

The chemical compositions measured by EA indicated that the sawdust consisted of C 46.09%, H 6.85%, O 35.09%, N 0.6%, and S 0.1% and small amounts of Cl, P, K, and Si. The chemical compositions measured by XRF indicate that the Palygorskite consists of SiO_2 55.10%, Al_2O_3 9.60%, Fe_2O_3 5.70%, Na_2O 0.05%, K_2O 0.96%, CaO 0.42%, MgO 10.70%, MnO 0.01%, and TiO_2 0.32%. Even small amounts of these compounds were found to be usable by microorganisms. There was no indication that heavy metals were related to the material analyzed here, indicating that heavy metals are appropriate for filter media and microbial growth.

3.3. Casting of thin section of PC

In a BAF system, packing media plays a significant role in effluent quality requirements. The granular medium is used in the composition of the biofilter beds for solid retention and solid–liquid separation. It is also the carrier of the biofilm. The characteristics of the filter media have significant impacts on the efficiency of wastewater treatment [42,43].

In order to obtain direct evidence of environmental microorganisms in porous structure of the PC, rubber casting experiments were used to generate quantitative size and shape data from pores in thin sections [35]. Fig. 4(a) shows the intergranular pore textures observed in the thin section. In Fig. 4(a), the black sections denote the calcined molded composite particles (calcined Palygorskite, calcined sawdust, and calcined sodium silicate) and gray ones represent the intergranular pores of PC. This demonstrates that PC has considerable internal porosity by volume. Guest microbes can be accommodated in these pores. The sizes of those interconnected pores are approximately 40–65 μm (Fig. 4(a) and 4(b)) and most bacteria are 0.5 μm or less in diameter. This allows these environmental microorganisms to achieve sustained population growth of population in the open porosity. When impregnated with blue-dyed epoxy (part d), fully interconnected porosity with a diameter of 60 μm can be determined from the white section (part c). In fact, blue-dyed epoxy in the porosity system must overcome the capillary resistance of the throat size before they enter porosity space indicating the narrow composition of the pores.

3.4. Applicability of PC and CAC in a BAF for municipal wastewater treatment

The two BAFs were monitored for 6 months after the start-up of the biofilters. Throughout the study, the two BAFs were operated at water temperatures ranging from 20 to 26˚C and DO > 4.00 mg/L. Four HRTs of 0.5, 1.75, 3.5, and 7 h were used.

3.5. Performance of TOC removal in the two BAFs

The average removal rates for TOC at different HRTs are shown in Table 5. These results suggest that

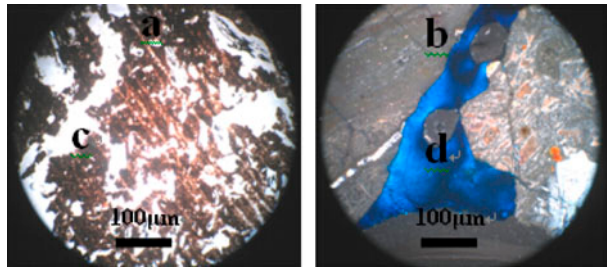

Fig. 4. Porosity of PC. (a) After calcination (gray-palygorskite); (b) filled (dark blue–open pores).

HRT has an impact on the overall TOC removal efficiency of PC media. One proposed explanation is that organic substrates were not fully degraded before being discharged from the BAF with shorter HRT. Shorter HRTs led to higher hydraulic loading and thus to stronger scouring on the surface of the medium. This causes lower biomass on the surface of the medium and thus lower TOC removal. Also, the increase in TOC load (i.e. HRT decreases) from the influent increases the rate of adsorption of the soluble organics into the microorganisms, which accelerates the first step in the removal organic matter by transporting these microorganisms from wastewater to the biofilm. The driving forces of biosorption have been reported to be electrostatic or hydrophobic interactions, which are greatly affected by the organic matter characteristics and mass transfer efficiencies [44–46]. As shown in Fig. 5, PC BAF showed a slightly higher TOC removal than CAC BAF. The main reason for this was that the surface and internal pore structure of PC is uniform and well developed. This allows soluble organic matter, nutrient substances, and suspended particles to reach the deep pores and increase the efficiency of mass transfer. The available space for microorganism growth, mass transfer of DO, and the opportunity for even dispersion of biomass were also increased by the extended infiltration of soluble pollutants into the deep holes in PC, which improved the effectiveness of biofiltration using the proposed material.

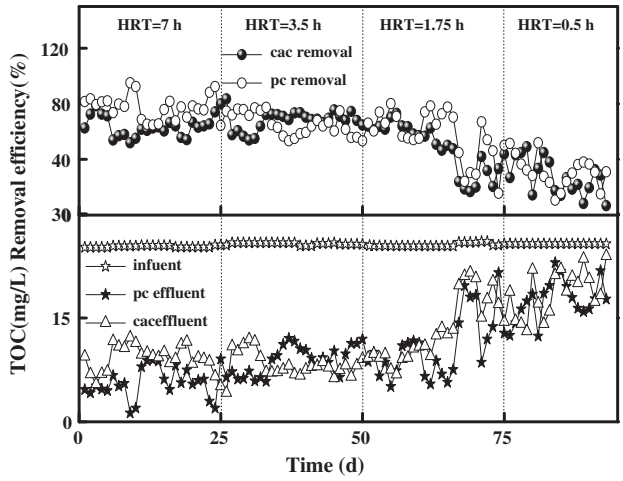

Fig. 5. Influent and effluent concentrations and removal efficiency of TOC over time.

3.6. Performance of NH_3-N removal in the two BAFs

As shown in Fig. 6, both BAFs had excellent NH_3-N removal when HRT was 7 h. From Table 5, it can be seen that when HRT was 0.5 h, NH_3-N was not fully nitrified before being discharged from the BAFs compared with longer HRTs. With a HRT of 0.5 h, the nitrobacteria did not have sufficient time to nitrify NH_3-N. The DO in the effluent at 0.5 h was slightly lower than that in systems with HRT longer than 1.75 h. Low DO in effluent could cause a slight decrease in the efficiency of the removal of NH_3-N. Finally, possible competition between heterotrophic bacteria and autotrophic bacteria in BAFs for the substrates, DO and inhabitation area could decrease its efficiency. A higher organic loading induced by the increase in hydraulic loading could favor heterotrophic bacteria over autotrophic bacteria [47,48]. As a result, nitrification was inhibited and NH_3-N removal decreased rapidly. As shown in Fig. 6, the PC BAF had a slightly higher rate of NH_3-N than CAC BAF. This could be due to the longer period of exposure

Table 5
Average removal rates of PC and CAC in BAF at different HRT

	TOC				NH_3-N				TN			
HRT (h)	0.5	1.75	3.5	7	0.5	1.75	3.5	7	0.5	1.75	3.5	7
Material												
PC	31.3	59.7	65.5	77.6	76.6	93	93	95.3	24.9	34.3	35.6	48.7
CAC	27.2	50.1	68	63.9	50.5	53.9	49.4	91.2	24.4	23.5	25.6	39.3
	NO_2-N				NO_3-N				PO_4^{3-}			
HRT (h)	0.5	1.75	3.5	7	0.5	1.75	3.5	7	0.5	1.75	3.5	7
Material												
PC	0.04	0.02	0.05	0.03	3.15	4.18	3.89	6.33	24.3	52.1	56.9	76.4
CAC	0.08	0.06	0.02	0.01	4.1	7.28	6.71	5.38	13.1	33	42.8	44.3

Notes: All values are average removal rates in %. NO_2-N and NO_3-N values are average effluent concentrations in mg/L.

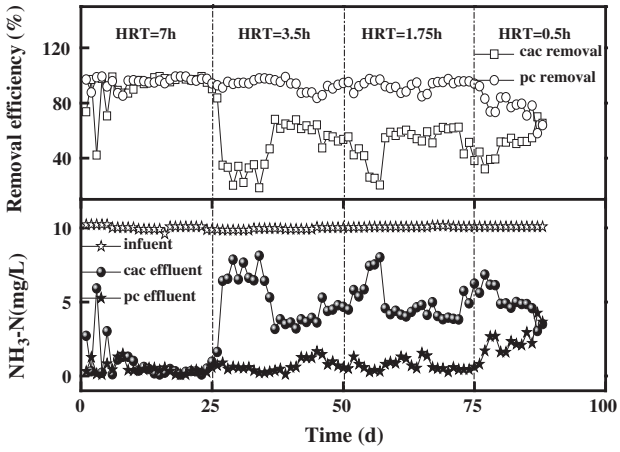

Fig. 6. Influent and effluent concentration and removal efficiency of NH_3-N over time.

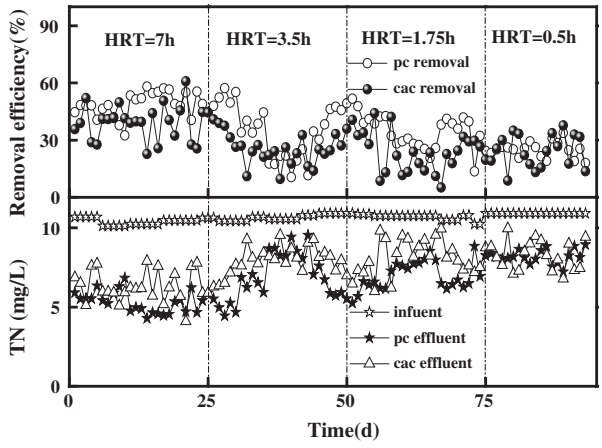

Fig. 7. Influent and effluent concentration and removal efficiency of TN over time.

from the HRT (7 h) where there was sufficient contact time to allow biomass to degrade NH_3-N in the BAFs. H^+ generated during nitrification in the PC BAF was easily removed due to the buffer capacity of PC, which produced a higher reduction of NH_3-N.

3.7. Performance of TN reduction in the two BAFs

As shown in Fig. 7 and Table 5, the removal efficiencies of TN increased in both biofilters as the HRT increased. The denitrification at HRT of 0.5 and 1.75 h was less efficient because denitrifying bacteria did not have sufficient time to denitrify NO_3-N.

As shown in Table 5, a high HRT (7 h) was necessary for efficient simultaneous nitrification and denitrification (SND). The TN removal performance of the PC BAF was slightly higher than that of CAC BAF. These results show that, under the same conditions, carrier biofilm layers with different levels of permeability (which is greatly affected by the porous structure of the PC), the contact-reaction potential of the microorganisms (nitrifiers and denitrifiers), and pollutants under anoxic conditions can affect nitrification and denitrification. These differences affect the microbial populations and activity levels in the biomass and adversely affect the efficiency of SND of the systems [49,50].

3.8. Concentration of NO_x-N at different HRT

As shown in Fig. 8, the overall concentration of NO_3-N was slightly higher in the PC effluent at HRT of 7 than in that of 3.5, 1.75, and 0.5 h. For CAC effluent, it was lower only with HRT of 0.5 h. NO_2-N in CAC effluent decreased slightly as HRT increased

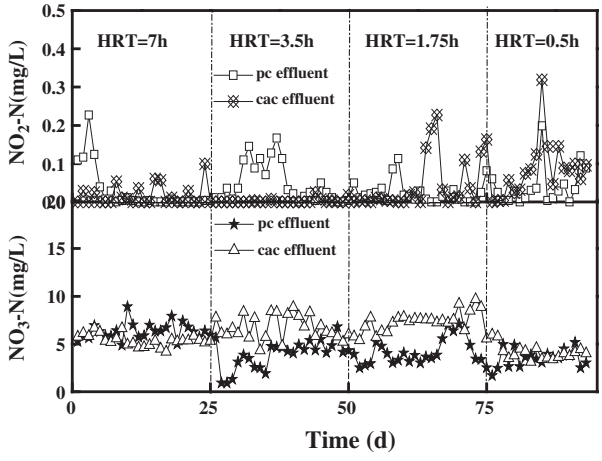

Fig. 8. Influent and effluent concentration of NO_x-N over time.

(lowest at 3.5 h), but PC effluent varied for each HRT. This is consistent with values given in Table 5. This indicates that nitrification, which is one of the limiting steps of the process, and oxidation of nitrite to nitrate were successful during the short contact time. However, limited denitrification was observed. This can be attributed to the overall removal of TN, which was less complete than removal of NH_3-N. Because denitrifiers use biological organic substrate as electron donors and NO_3-N as electron acceptors, a reduction in the NO_3-N concentration was expected, but it instead had an increasing trend in the HRT tested [51,52]. The limited denitrification can be attributed to the lower alkalinity, which was due to the release of H^+ ions during the nitrification phase [53].

3.9. Performance of PO_4^{3-} reduction in the two BAFs

In terms of PO_4^{3-} removal, the rates at different HRT can be seen in Table 5 and Fig. 9, where the PC BAF displayed more efficient PO_4^{3-} removal than CAC BAF. One proposed explanation is that higher phosphate sorption capacity can be achieved on PC from thermal activation. Major changes in the crystal structure of Palygorskite, including more calcium, iron, and aluminum can be released from the crystal matrix at 700℃, which promoted phosphorus sorption. Precipitation of calcium/iron/aluminum phosphate produced in the PC BAF during the process could be a indicative of phosphate removal although these three precipitate solubility products have very small: Ksp $(Ca_3(PO_4)_2 = 1.40 \times 10^{-37}$, Ksp$(FePO_4) = 9.91 \times 10^{-16}$, Ksp$(AlPO_4) = 6.3 \times 10^{-19}$. Another proposed explanation is that some of the microbial nutrient requirements necessary to maintaining life and growth were met with the removal of phosphorous. Nutrients required by microorganisms include the following: CO_2, HCO_3^-, trace elements, and organic compounds required for the synthesis of the cytoplasm and organic and inorganic compounds for cell growth and biosynthetic reactions. In this case, the phosphorus was removed mainly nutritional consumption by microorganisms. The biofilm biomass was 34.1 mg TN/g for PC and 2.2 mg TN/g for CAC. A higher biomass value indicates more bacteria being produced

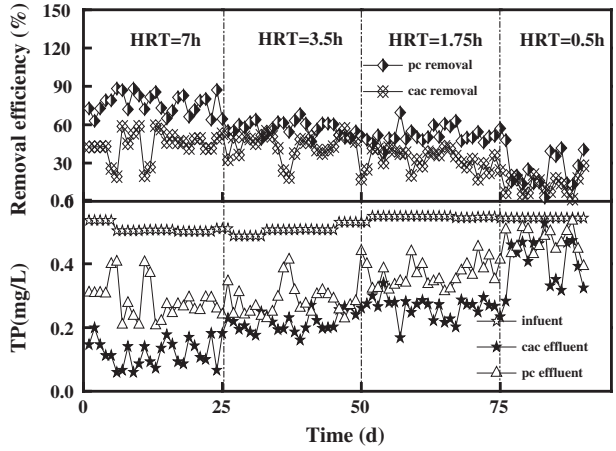

Fig. 9. Influent and effluent concentration and removal efficiency of PO_4^{3-} over time.

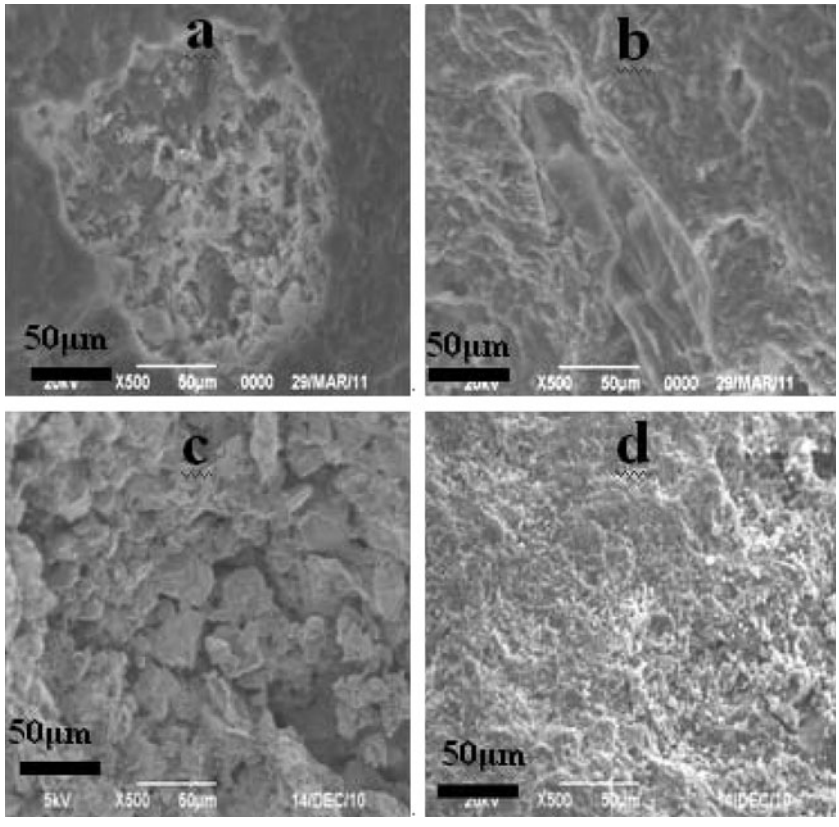

Fig. 10. SEM images of internal and external surface in PC/CAC. (a), raw external surface of PC; (b), raw internal surface of PC; (c), raw external surface of CAC; (d), raw internal surface of CAC.

from phosphate removal, although its absorption is small. This leads to a third proposed explanation, in which the PC has more specific surface area (61 m^2/g) than CAC (2 m^2/g). This can lead to a greater rate of phosphate removal via media adsorption. When the as-synthesized PC was heated above 700˚C, most of the hydroxyls were removed and aluminum was activated and exposed at the surface. Activated Al atoms showed considerable affinity for phosphate and may provide active sites for phosphate adsorption [26,41].

Based on the analysis described above, the adsorption of phosphate in the PC was the most likely explanation because the microbial phosphorus absorption and precipitation of calcium/iron/aluminum phosphate produced in the PC was very small.

4. Scanning electron microscopy (SEM) analysis.

Several SEM images for the ordered structure and biomass growth of PC and CAC are shown in Fig. 10. In Fig. 10(a), the appearance of rough surface on PC is described as the coral-like porosity structure that provides shelter from the wastewater shear forces. The microstructure of the internal cross section of the PC is shown in Fig. 10(b). It also indicates that the prepared PC has a high porosity with open, rectangular pores, as shown in Fig. 10(a) and (b). Macropores form inside the particles when sawdust is calcined during sintering. High porosity from PC media is suitable for the use as biomedium in BAF reactors. The micrograph of CAC clearly shows pores with diameters ranging 6.0–10.0 μm irregularly distributed on the surface (Fig. 10(c)). There are some small pores and smooth surfaces visible in Fig. 10(d).

The SEM images of the PC after use in the BAF reactor are illustrated in Fig. 11(a) and (b). The biofilm was found to overlay the surface of the PC. As shown in Fig. 11(a), there were two kinds of biological bacteria, filamentous and chain shaped. After the growth of bacterial population, a biofilm was clearly visible on the surface of internal pores (Fig. 11(b)). At the start-up phase of the BAF reactor, the biofilms first

Fig. 11. SEM images of internal and external surface in PC/CAC after microbial load. (a), microbial load on external surface of PC; (b), microbial load on internal surface of PC; (c), microbial load on external surface of CAC; (d), microbial load on internal surface of CAC.

developed when some bacteria became irreversibly attached to the PC. Until more metabolite grew the PC surface, the PC was completely covered with biofilms distributed randomly on the surface. The microstructure in Fig. 11(c) and (d) suggests that a small number of microorganisms were immobilized on the inner and outer surfaces of pores in CAC.

4.1. Microscopic observation for protozoan and metazoan populations in biofilm

The optical microscopic observation (conducted at HRT of 7 h) in Fig. 12 shows that protozoan and metazoan organisms were visible in the biofilm. These mainly included *Opercularia* sp., *Paramecium* sp., and nematodes. Protozoa are well-known indicators of the good performance of biological wastewater treatment systems. The stable existence of protozoans and metazoans can also contribute to CAC and PC reduction [54,55]. The dominant species in the CAC and PC biofilters are nematodes, *Paramecium* sp., *Epistylis* sp. (or *Opercularia* sp.), and *Aeolosoma hemprichi* (big body). The differences in the predominant populations in the two systems indicated a relationship between the CAC and PC characteristics and the growth state of protozoa and metazoan in the biofilm. Accumulation of abundant micro-animals on the surface and pores of PC indicated that the gradual filling of organic matter and other substrates to the pore spaces was efficient and speedy [56]. This can be attributed to the interconnected porous structures of PC compared to CAC.

4.2. Determination of biomass in media.

The biomass of grown biofilm was determined to assess the performance of PC and CAC in the BAF reactor [32]. The biofilm biomass was 34.1 mg TN/g for PC and 2.2 mg TN/g for CAC. A higher biomass indicates more bacteria available to perform TOC, NH_3-N, TN, and phosphate removal. The structural and morphological characteristics of the porous media, as shown in Figs. 10 and 11, proved that PC surface

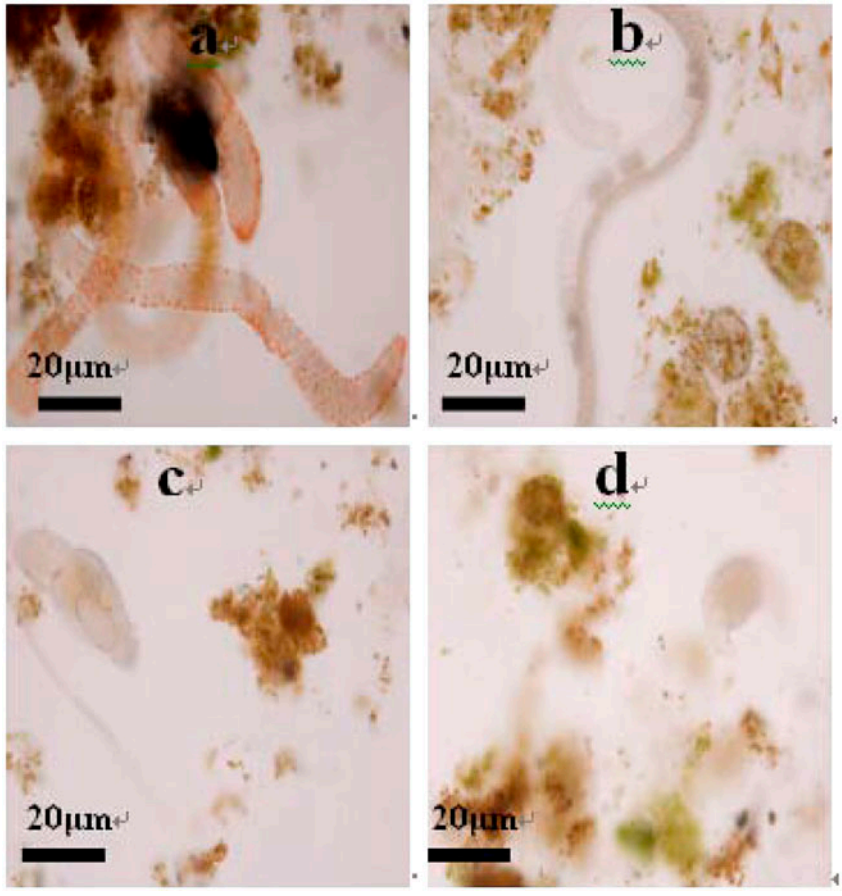

Fig. 12. Microscopic observation of protozoans and metazoans in the systems. (a–CAC; b–PC; c–PC; d–PC).

and internal pores were advantageous to microbial growth under the conditions tested.

5. Conclusions

Based on the results obtained, the following conclusions can be drawn:

The optimum mass ratio of Palygorskite, sawdust, and sodium silicate for the preparation of PC is 10:2:1 with sintering at 700˚C for 180 min. The specific surface area of PC was 61 m^2/g, with a porosity of 67% and a compressive strength range of 50–58 N. The specific surface area of CAC was 2 m^2/g. The parameters obtained with PC were higher than those obtained for CAC. SEM and porosimetry results suggest that the uniform and interconnected pores in PC are suitable for microbial growth. This was confirmed when more biomass was produced using PC media than using CAC. The efficiency of the BAF reactor was higher with PC than with CAC in terms of TOC, TN, P, and NH_3-N removal under the conditions tested.

A more favorable environment for nitrifying bacteria was provided in the biofilter with PC. PC BAFs can therefore be considered a novel and viable process for treating wastes with wastes and provide a promising use for sawdust waste material.

The results indicate that PC BAF had the highest adsorption capacity. Results showed that the PC BAF had a slightly higher P removal rate than CAC BAF. This was due to changes in the crystal structure of PC after thermal treatment at 700˚C where activated Al from the dehydroxylation process became exposed. All of these structural changes increased the adsorption capacity of PC, in particular, for phosphate removal.

Acknowledgements

The authors would like to thank the financial support from the National Natural Science Foundation of China (NSFC: 41102023, 41072036, 41130206).

References

[1] N.R. Louzeiro, D.S. Mavinic, W.K. Oldham, Methanol-induced biological nutrient removal kinetics in a full-scale sequencing batch reactor, Water Res. 36 (2002) 2721–2732.

[2] D. Obaja, S. Macé, J. Costa, Nitrification, denitrification and biological phosphorus removal in piggery wastewater using a sequencing batch reactor, Bioresour. Technol. 87 (2003) 103–111.

[3] M.E. Kvarnström, C.A.L. Morel, T. Krogstad, Plant-availability of phosphorus in filter substrates derived from small-scale wastewater treatment systems, Ecol. Eng. 22 (2004) 1–15.

[4] L. Holakoo, G. Nakhla, A.S. Bassi, Long term performance of MBR for biological nitrogen removal from synthetic municipal wastewater, Chemosphere 66 (2007) 849–857.

[5] Q. Feng, A.F. Yu, L.B. Chu, X.-H. Xing, Performance study of the reduction of excess sludge and simultaneous removal of organic carbon and nitrogen by a combination of fluidized- and fixed-bed bioreactors with different structured macroporous carriers, Biochem. Eng. J. 39 (2008) 344–352.

[6] S.-B. He, G. Xue, H.-N. Kong, The performance of BAF using natural zeolite as filter media under conditions of low temperature and ammonium shock load, J. Hazard. Mater. 143 (2007) 291–295.

[7] R.F. Goncalves, F. Rogalla, Continuous biological phosphorus removal in a biofilm reactor, Water Sci. Technol. 26 (1992) 2027–2030.

[8] S. Li, J. Cui, Q. Zhang, J. Fu, J. Lian, C. Li, Performance of blast furnace dust clay sodium silicate ceramic particles (BCSCP) for brewery wastewater treatment in a biological aerated filter, Desalination 258 (2010) 12–18.

[9] D.L. Su, J.L. Wang, K.W. Liu, Z. Ding, Kinetic performance of oil-field produced water treatment by biological aerated filter, Chin. J. Chem. Eng. 15 (2007) 591–594.

[10] F. Osorio, E. Hontoria, Wastewater treatment with a double-layer submerged biological aerated filter, using waste materials as biofilm support, J. Environ. Manage. 65 (2002) 79–84.

[11] L.P. Qiu, J. Ma, L.X. Zhang, Characteristics and utilization of biologically aerated filter backwashed sludge, Desalination 208 (2007) 73–80.

[12] R.E. Moore, J. Quarmby, T. Stephenson, BAF media: Ideal properties and their measurement, Process Saf. Environ. Prot. 77 (1999) 291–297.

[13] L. Mendoza-Espinosa, T. Stephenson, A review of biological aerated filters (BAFs) for wastewater treatment, Environ. Eng. Sci. 16 (1999) 201–206.

[14] H.D. Stensel, R.C. Brenner, K.M. Lee, Biological aerated filter evaluation, J. Environ. Eng. 114 (1988) 655–671.

[15] Y.Z. Yu, Y. Feng, L.P. Qiu, Effect of grain-slag media for the treatment of wastewater in a biological aerated filter, Bioresour. Technol. 99 (2008) 4120–4123.

[16] M. Rozic, S.C. Stefanonvic, S. Kuranjica, et al., Ammoniacal nitrogen removal from water by treatment with clays and zeolites, Water Res. 34 (2000) 3675–3681.

[17] X.J. Xiong, Z.L. Ye, Comparison of nitrification behavior between shell and plastics ball carrier in aerated biofilter, J. Xiamen Univ . (Nat. Sci.) 44 (2005) 538–541.

[18] Y.J. Shen, G.X. Wu, Y.B. Fan, Performances of biological aerated filter employing hollow fiber membrane segments of surface-improved poly (sulfone) as biofilm carriers, J. Environ. Sci. 19 (2007) 811–817.

[19] Y.-X. Liu, D.-X. Yuan, T.O. Yang, Study of municipal wastewater treatment with oyster shell as biological aerated filter medium, Desalination 254 (2010) 149–153.

[20] S. Han, Q. Yue, M. Yue, The characteristics and application of sludge-fly ash ceramic particles (SFCP) as

novel filter media, J. Hazard. Mater. 171 (2009) 809–814.
[21] P.H. Hsu, Precipitation of phosphate from solution using aluminum salt, Water Res. 9 (1975) 1155–1161.
[22] Q.H. Huang, Z.J. Wang, D.H. Wang, Origins and mobility of phosphorus forms in the sediments of lakes Taihu and Chaohu, China, J. Environ. Sci. Health. Part A Toxic/Hazard. Subst. Environ. Eng. 40 (2005) 91–102.
[23] Bradley, The structural scheme of attapulgite, Am. Mineral. 25 (1940) 405–410.
[24] Y.W. Chen, B.Q. Qin, K. Teubner, M.T. Dokulil, Long-term dynamics of phytoplankton assemblages: Microcystis-domination in Lake Taihu, a large shallow lake in China, J. Plankton Res. 25 (2003) 445–453.
[25] F. Gan, J. Zhou, H. Wang, Removal of phosphate from aqueous solution by thermally treated natural Palygorskite, Water Res. 43 (2009) 2907–2915.
[26] H. Ye, F. Chen, Y. Sheng, Adsorption of phosphate from aqueous solution onto modified Palygorskites, Sep. Purif. Technol. 50 (2006) 283–290.
[27] E. Salehi, J. Abedi, T. Harding, Bio-oil from sawdust: Pyrolysis of sawdust in a fixed-bed system, Energy Fuels 23 (2009) 3767–3772.
[28] G.D. Ji, Y. Zhou, J.J. Tong, Nitrogen and phosphorus adsorption behavior of ceramsite material made from coal ash and metallic iron, Environ. Eng. Sci. 27 (2010) 871–878.
[29] X.X. Lu, J.M. Song, X.G. Li, H. Yuan, T. Zhan, N. Li, X. Gao, Geochemical characteristics of nitrogen in the southern Yellow Sea surface sediments, J. Mar. Sys. 56 (2005) 17–27.
[30] Y. Feng, Y. Yu, L. Qiu, X. Wan, L. Chen, Performance of water quenched slag particles (WQSP) for municipal wastewater treatment in a biological aerated filter (BAF), Biomass Bioenergy 45 (2012) 280–287.
[31] Chinese Mohurd, Artifical Ceramsite Filter Material for Water Treatment, China Standard Publishing House, Beijing, China, 2008.
[32] Y.R. Zhu, R.Y. Zhang, F.C. Wu, Distribution of bioavailable nitrogen and phosphorus forms and their relationship in the sediments of Dianchi Lake, Res. J. Environ. Sci. 8 (2010) 994–998. (in Chinese).
[33] Y. Yanzhen, Z. Chunhui, F. Yan, Preparation and performance test of composite clinoptilolite filter materials, Chin. J. Environ. Eng. 10 (2010) 2208–2210.
[34] Yu Yan Zhen, Feng Yan, Qiu Li Ping, W. Han, L. Guan, Effect of grain slag media for the treatment of wastewater in a biological aerated filter, Bioresour. Technol. 99 (2008) 4120–4123.
[35] Sandstone pore structure method of image analysis (Industry standard CJ/T) (in Chinese).
[36] Chinese E.P.A, State Environmental Protection Administration of China, Monitoring and Analysis Methods of Water and Wastewater, fourth ed., Environment Science, Beijing, 2002.
[37] C.Y. Wu, S. Ushiwaka, H. Horii, K. Yamagiwa, Membrane-attached biofilm as a mean to facilitate nitrification in activated sludge process and its effect on the microfaunal population, Biochem. Eng. J. 40 (2008) 430–436.
[38] E. Ramirez-Lopez, J.C. Hernandez, L. Dendooven, P. Rangel, F. Thalasso, Characterization of five agricultural by-products as potential biofilter carriers, Bioresour. Technol. 88 (2003) 259–263.
[39] Y.F. Shen, Z.S. Zhang, Modern Biomonitoring Techniques using Freshwater Microbiota, China Architecture & Building Press, Beijing, China, 1990 (in Chinese).
[40] G.R. Xu, J.L. Zou, Y. Dai, Utilization of dried sludge for making ceramsite, Water Sci. Technol. 54 (2006) 69–79.
[41] J. Xie, T. Chen, C. Qing, Adsorption of phosphate from aqueous solutions by thermally modified Palygorskite, Environ. Eng. Manage. J. 12 (2013) 1393–1399.
[42] S. Han, Q. Yue, M. Yue, B. Gao, Q. Li, H. Yu, Y. Zhao, Y. Qi, The characteristics and application of sludge-fly ash ceramic particles (SFCP) as novel filter media, J. Hazard. Mater. 171 (2009) 809–814.
[43] A. Patel, J. Zhu, G. Nakhla, Simultaneous carbon, nitrogen and phosphorous removal from municipal wastewater in a circulating fluidized bed bioreactor, Chemosphere 65 (2006) 1103–1112.
[44] K. Nootong, W.K. Shieh, Analysis of an upflow bioreactor system for nitrogen removal via autotrophic nitrification and denitrification, Bioresour. Technol. 99 (2008) 6292–6298.
[45] T. Osaka, K. Shirotani, S. Yoshie, S. Tsuneda, Effects of carbon source on denitrification efficiency and microbial community structure in a saline wastewater treatment process, Water Res. 42 (2008) 3709–3718.
[46] F. Liu, C.C. Zhao, D.F. Zhao, G.H. Liu, Tertiary treatment of textile wastewater with combined media biological aerated filter (CMBAF) at different hydraulic loadings and dissolved oxygen concentrations, J. Hazard. Mater. 160 (2008) 161–167.
[47] Y. Feng, Y. Yu, Q. Duan, J. Tan, C. Zhao, The characteristic research of ammonium removal in grain-slag biological aerated filter (BAF), Desalination 263 (2010) 146–150.
[48] C.K. Choi, J.K. Lee, K.H. Lee, The effects on operation conditions of sludge retention time and carbon/nitrogen ratio in an intermittently aerated membrane bioreactor (IAMBR), Bioresour. Technol. 99 (2008) 5397–5401.
[49] Z.M. Fu, F.L. Yang, F.F. Zhou, Y. Xue, Control of COD/N ratio for nutrient removal in a modified membrane bioreactor (MBR) treating high strength wastewater, Bioresour. Technol. 100 (2009) 136–141.
[50] Y.Z. Li, Y.L. He, D.G. Ohandja, J. Ji, Simultaneous nitrification–denitrification achieved by an innovative internal-loop airlift MBR: Comparative study, Bioresour. Technol. 99 (2008) 5867–5872.
[51] K.A. Third, B. Gibbs, M. Newland, Long-term aeration management for improved N-removal via SND in a sequencing batch reactor, Water Res. 39 (2005) 3523–3530.
[52] Y.C. Chiu, L.L. Lee, C.N. Chang, A.C. Chao, Control of carbon and ammonium ratio for simultaneous nitrification and denitrification in a sequencing batch bioreactor, Int. Biodeterior. Biodegrad. 59 (2007) 1–7.
[53] Q. Yang, Y.Z. Peng, X.H. Liu, W. Zeng, T. Mino, H. Satoh, Nitrogen removal via nitrite from municipal wastewater at low temperatures using real-time control to optimize nitrifying communities, Environ. Sci. Technol. 41 (2007) 8159–8164.
[54] M. Martín-Cereceda, B. Pérez-Uz, S. Serrano, Dynamics of protozoan and metazoan communities in a full scale wastewater treatment plant by rotating biological contactors, Microbiol. Res. 156 (2001) 225–238.

[55] L.W. Xiao, M. Rodgers, J. Mulqueen, Organic carbon and nitrogen removal from a strong wastewater using a denitrifying suspended growth reactor and a horizontal-flow biofilm reactor, Bioresour. Technol. 98 (2007) 739–744.

[56] J.L. Zou, G.R. Xu, K. Pan, Nitrogen removal and biofilm structure affected by COD/NH_4^+–N in a biofilter with porous sludge-ceramsite, Sep. Purif. Technol. 94 (2012) 9–15.